EISSN: 2707-0425

East African Journal of Science, Technology and Innovation, Vol. 5 (Special issue): December 2024

First-principles investigations into the characteristic properties of corundum samples from the Arusha region

[1]TARIMO E J., [1] P V K RAO., [1]MWANGA S F*

[1]Department of Physics, The University of Dodoma, Dodoma, Tanzania

***Corresponding Author**: esthertarimoj@gmail.com*

Abstract

Understanding the characteristic properties of corundum gemstone is essential for its use in gemstone treatment, as well as in various other industries. Corundum samples obtained from the Arusha mining region were analyzed for crystallographic data using XRD analysis. This crystallographic data is then utilized to construct the crystal structure of the samples in the Biovia Materials Studio modeling and simulation software. The electronic, optical, and elastic properties of the selected sample are explored using the plane wave approach within the framework of the first-principles density functional theory (DFT), implying the Cambridge Serial Total Energy Package (CASTEP) code with Generalized Gradient Approximations and the Perdew-Burke-Ernzerhof exchange-correlation functional. For the calculations, a sampling mesh of 6×6×2 k-points, with the cut-off energy of 600 eV, and the total energy convergence within 1.0 x 10-5 eV/atom is used. The band gap determined is 6.13 eV at the gamma point which is in concurrence with the previous values from the literature. The polarized optical properties of the structure were studied and visualized by plotting their directional dependencies. The reflectivity spectra exhibited isotropic behavior in the ultraviolet range with a maximum peak at 52.24 nm along [001], [010], and [100] directions. Also, the absorption peak is observed around 65.59 nm along [001], [010], and [100] directions. Pugh's ratio suggests that the sample is deemed brittle with a ratio of 0.65 as G/B > 0.5. The calculated Poisson's ratio is 0.23 indicating the dominant covalent bond. The results indicate that the investigated sample is a suitable insulator, brittle, and displays isotropic optical reflectivity.

Keywords: *First-Principles studies; Corundum; Band gap; Polarized; Anisotropic Reflectivity; Elasticity*

Received: 17/01/24
Accepted: 12/03/24
Published: 20/12/24

Cite as, *Tarimo et al., (2024). First-principles investigations into the characteristic properties of corundum samples from the Arusha region. East African Journal of Science, Technology and Innovation 5(Special issue).*

Introduction

Corundum gemstone is a rock-forming mineral that consists primarily of aluminum oxide (Al_2O_3). Along with aluminum and oxygen, it may contain small amounts of other elements as impurities which can alter its color and other properties. Typical impurities in corundum include iron, chromium, titanium, and vanadium. These impurities can create different colored varieties of corundum, such as ruby (red) and sapphire (blue) (Aggarwal & Ramdas, 2019). The precise chemical composition of corundum can differ based on its source and location yet aluminum oxide always remains its primary component (Keulen et al., 2020). Sri Lanka, Myanmar, Tanzania, Kenya, Madagascar, Australia, and Mozambique, are among the nations that have significant natural corundum resources (Mansoor et al., 2021).

Tanzania, on the other hand, is noted for being home to a large corundum reserve (Park, 2004). Corundum can be identified through its physical, optical, electrical, mechanical, and chemical properties. Due to its valuable applications, researchers have developed an interest in studying it by employing both theoretical and experimental methods. It is vital to comprehend the characteristic properties, as they are a well-known necessity for their technological applications. The corundum gemstone's properties are useful for applications by gemologists, the stone industry, manufacturing industries, and the medical field (Raisin et al., 2021).

The atomistic level for understanding the electronic structure is now possible due to advancements in density functional theory (DFT) that are possible by computational calculations (Ozaki et al., 2021). The best method for condensed matter to explore several material properties is by using DFT calculation. The plane wave pseudopotential approach, which derives the properties of materials from their fundamental principles, is used to compute the DFT using the Cambridge Serial Total Energy Package (CASTEP). Numerous material properties, such as energetics, electrical response properties, vibrational properties, and atomic-level structure, can be simulated using computational methods (Kovilpalayam et al., 2022). The work aims to investigate the characteristic properties of corundum from the Arusha region using the first principles studies. In this present study, the corundum samples collected from the Arusha mining region were characterized by using XRD analysis, and the information obtained from the XRD analysis was used to investigate electronic, optical, and elastic properties by first-principles density functional theory.

Materials and Methods

The experiment was conducted on a commercial corundum sample obtained from Mundarara mine, Longido District in Arusha region, Tanzania. At ambient temperature, using a Bruker AXS D76187 X-ray powder diffractometer in a step-scanning setting, using a Cu pipe with λ = 1.540598 with an average scanning step of 0.02° (2θ) and an estimation time of 0.15 s per step, the diffraction lines of the samples were captured within an interval of 5°–65° (2θ) and recorded. Ab initio was performed using the density functional theory (DFT) applying the Cambridge Sequential Total Energy Package (CASTEP) computer program together with the generalized gradient approximation (GGA), with the Perdew-Burke-Ernzerhof (PBE) exchange-correlation functional (Clark et al., 2005; Perdew et al., 1996). The convergence tolerances designated for all geometry optimization in the BFGS minimization scheme (Fischer & Almlof, 1992) were set as ultrafine quality and a sampling mesh of 6×6×2 special Monkhorst-Pack k-points, with the cut-off energy of 600 eV and a total energy convergence within 1.0×10^{-5} eV/atom was implemented to guarantee correct overall energy convergence (Vanderbilt, 1990). For the pseudopotential configurations, $1s^2\ 2s^2\ 2p^6\ 3s^2\ 3p^1$ electrons for Al atom and $1s^2\ 2s^2\ 2p^4$ electrons for O atoms were implemented.

A thorough comprehension of the electronic structure of materials is provided by optical functions such as the absorption coefficient, α(ω); refractive index, $n(\omega)$; the extinction coefficient, k(ω); reflectivity, R(ω); and energy loss function, L(ω) (Karazhanov et al., 2007). The dielectric function, which describes an electronic system's linear response when an external electric field is present is given by equation (2) as used elsewhere (Khireddine et al., 2021). The dielectric function is a useful parameter for characterizing the optical properties of materials.

$$\mathcal{E}(\omega) = \mathcal{E}_1(\omega) + i\mathcal{E}_2(\omega) \qquad (2)$$

Where: $\mathcal{E}_1(\omega)$ is the real part and $\mathcal{E}_2(\omega)$ is the imaginary part. The real $\mathcal{E}_1$ and imaginary $\mathcal{E}_2$ parts are calculated using equations (3) and (4). These values are important because all other parameters of optical properties can be deduced from those two values as presented in equations (5) – (9) also described elsewhere (Heiba et al., 2020):

$$\mathcal{E}_1(\omega) = 1 + \frac{2p}{\pi}\int_0^{\infty} \frac{\omega \cdot}{\omega^{0.2} - \omega^2} d\omega \cdot \quad (3)$$

$$\mathcal{E}_2(\omega) = \frac{2\omega p}{\pi}\int_0^{\infty} \frac{\mathcal{E}_1 - 1}{\omega^{0.2} - \omega^2} d\omega \cdot \quad (4)$$

$$\alpha(\omega) = \sqrt{2\omega}\sqrt{(\mathcal{E}_1^2 + \mathcal{E}_2^2)^{1/2} - \mathcal{E}_1} \quad (5)$$

$$n(\omega) = \sqrt{\frac{\mathcal{E}_r(\omega)}{2} + \frac{(\mathcal{E}_r^2(\omega) + \mathcal{E}_i^2(\omega))^{1/2}}{2}} \quad (6)$$

$$k(\omega) = \sqrt{\frac{-\mathcal{E}_r(\omega)}{2} + \frac{(\mathcal{E}_r^2(\omega) + \mathcal{E}_i^2(\omega))^{1/2}}{2}} \quad (7)$$

$$R(\omega) = \frac{(n-1)^2 + K^2}{(n+1)^2 + K^2} \quad (8)$$

$$L(\omega) = \frac{\mathcal{E}_2(\omega)}{\mathcal{E}_1^2(\omega) + \mathcal{E}_2^2(\omega)} \quad (9)$$

Electronic, optical, and elastic properties were computed based on the results obtained from the experiment by using density functional theory the way it is employed in CASTEP with the PBE technique. The evaluation of the sample's electrical, optical, and elastic characteristics was then compared with both experimental and theoretical findings.

Results

Structural parameters

From XRD analysis the selected sample from the Arusha mining site is observed to have a space group of R 3 c and the rhombohedral unit cell with 10 atoms (two Al_2O_3 formula units) as it is observed in Figure 1(c), these results are similar from the one of (Godin & LaFemina, 1994). The lattice parameters are described in Table 1 with the positions of atoms (0.1456, 0.145, 0.145) and (-0.053, 0.25, 0.553) for Al and O, respectively. Figure 1(a) depicts the XRD patterns for experimental and simulation as observed from the same 2θ degree.

Table 1

Structural parameters of the selected samples

Rhombohedral	Experimental Values	Optimized values
a (Å)	5.1280	5.155
a (Degree)	55.270	55.106
D (g/cm^2)	4.166	3.9451
V (Å^3)	84.870	85.834

Electronic Properties

In Figure 2, it is evident that the Arusha corundum exhibited a direct bandgap of 6.13 eV at the gamma point. It is worth noting that this value lies within a variety of prior discoveries and experimental values of 6 eV – 9.5 eV (Zainullina & Korotin, 2020). Furthermore, Figure 3(b & c) illustrates the comprehensive density of state contributions arising from O2p (-7.07 - 0 eV), Al3s (6.13 - 18.88 eV), and Al3p (6.51 - 19.89 eV).

Optical properties

Figure 4(a & b) shows the dielectric function spectra of the real ($\mathcal{E}_1$) and imaginary ($\mathcal{E}_2$) sections of the dielectric characteristics, respectively. As observed from Figure 4(a) the real part of dielectric absorption, has a maximum peak at 9.75 eV and a minimum peak at 19.12 eV. The static dielectric constant ε_1 (0) is determined when the frequency is zero, which is linked with the bandgap. From this, the ordinary refractive index can be calculated as given in equation (1).

$$n(0) = \varepsilon(0)^{1/2} \quad (1)$$

Figure 5 represents the variations of reflectivity, absorption coefficient, and loss function. As it is depicted in Figure 5(a), the maximum peak of reflectivity is at 52.24 nm along [001], [010], and [100] directions. Figure 5(b) indicates the maximum peak of absorption coefficient around 65.59 nm along [001], [010] and [100] directions. There is another peak observed at 74.28 eV along [001], [010], and [100] directions.

Figure 1

(a) XRD pattern from the experiment (b) XRD pattern from simulation (c) Corundum's crystal structure in rhombohedral lattice from Arusha Sample

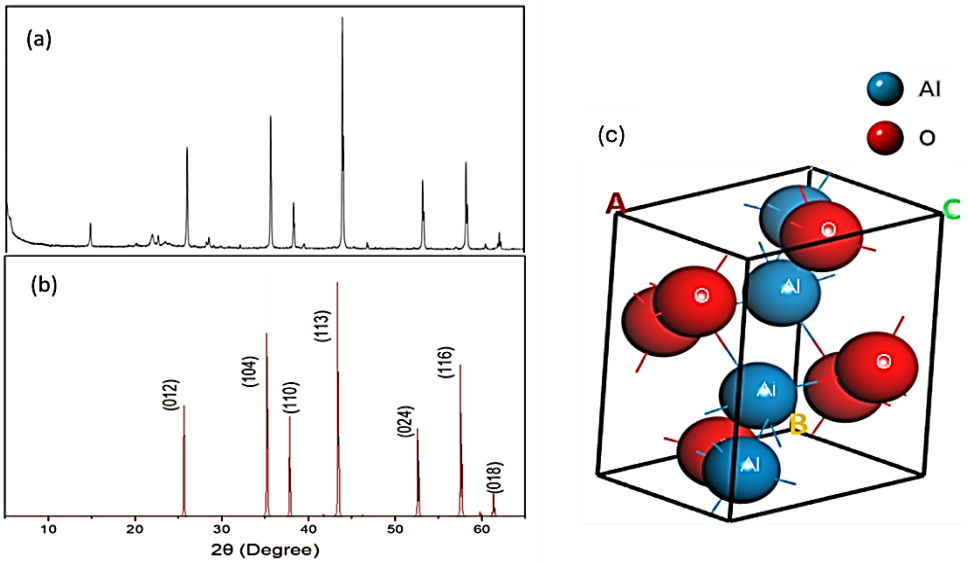

Figure 2

(a) Band structure and (b) Density of states from Arusha Sample

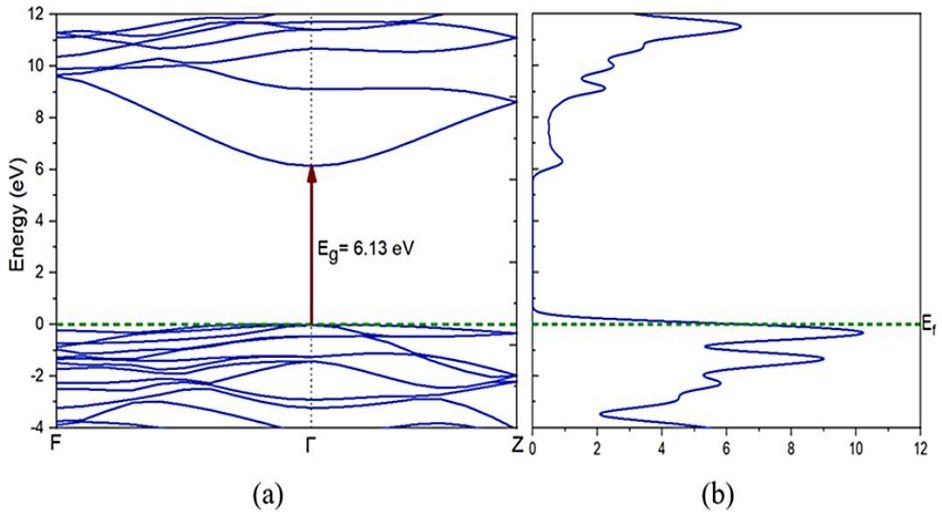

Figure 3

(a) Total density of state (b) O-Partial density of state and (c) Al-Partial density of States

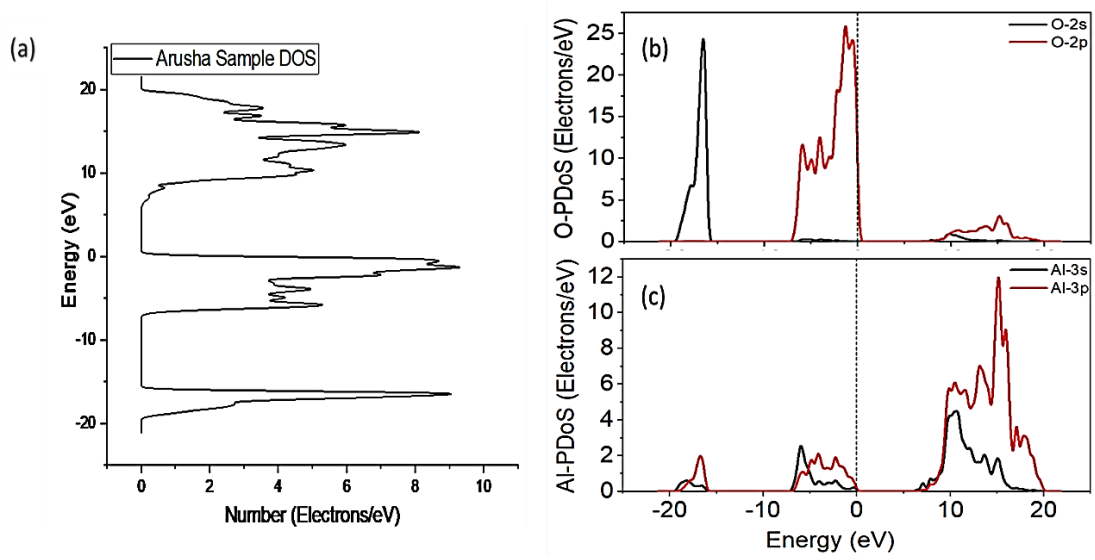

Figure 4

(a) Real part of dielectric function (b) Imaginary part of dielectric function (c) Refractive index and (d) Extinction coefficient

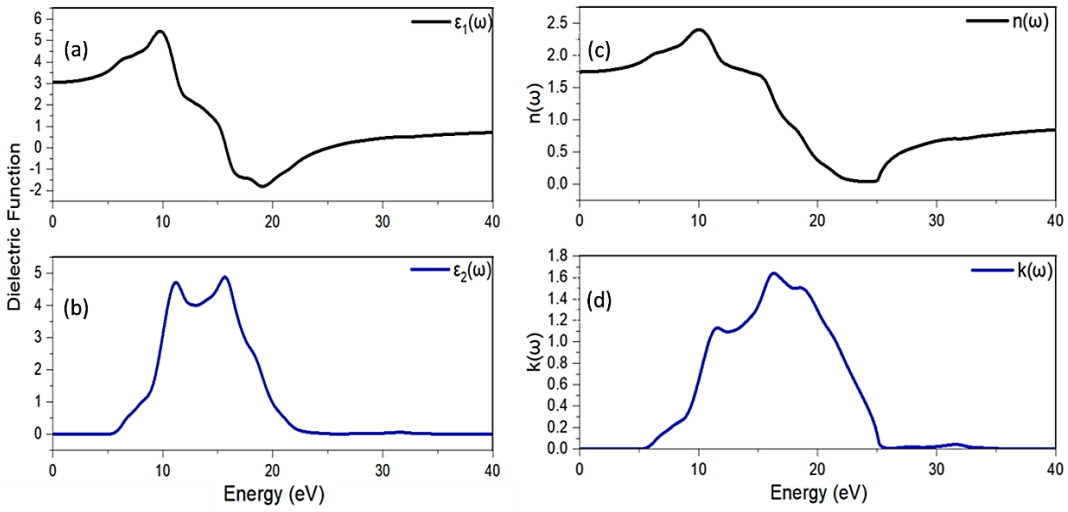

Figure 5

(a) Reflectivity (b) Absorption coefficient and (c) Loss function

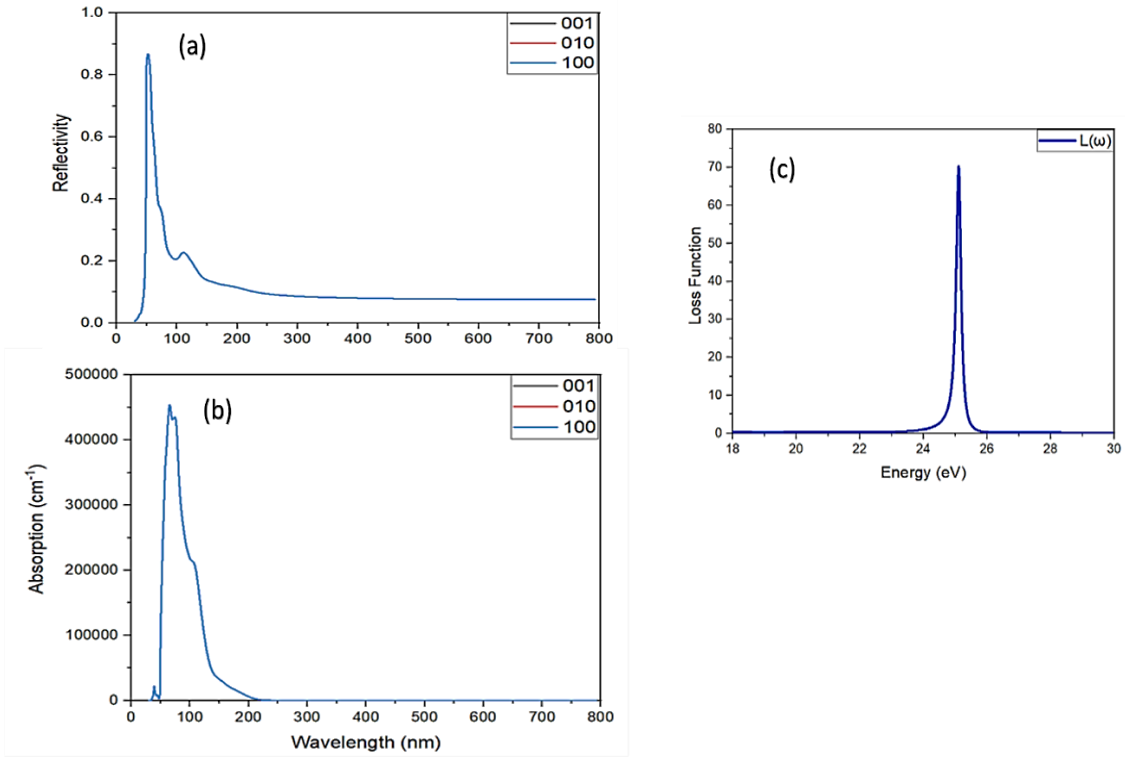

Elastic properties

The components of the elastic stiffness tensor C_{11}, C_{12}, C_{13}, C_{33}, and C_{44} that characterize the elastic behaviors of the crystalline material, and are critical in understanding how material deforms under stress were compared as described in Table 2.

Table 2

Comparison of elastic stiffness constants C_{ij} (in GPa), and modulus of elasticity for the selected corundum sample with the literature values

Parameter	Arusha sample	Chihi et al., 2019	Heiba et al., 2020b
C_{11}	445	468	449
C_{12}	147	150	148
C_{13}	102	105	103
C_{14}	19	24	-
C_{33}	450	476	456
C_{44}	135	140	135
B	226	237	229
G	148	153	148
Y	364	435	421
G/B	0.65	0.65	0.64
v	0.23	0.19	0.41

Discussion

Electronic and optical properties

The XRD patterns generated by Material Studio (simulated results) in Figure 1(b) closely resemble the experimental ones in Figure 1(a), with minor variations in the small peaks detected by XRD. These small peaks in the XRD patterns could be due to background noise, indicating the presence of trace amounts of other metal constituents in the sample. In contrast, the Material Studio simulation was based on pure corundum samples.

One way to understand the changes in state occupancy across various energy intervals is through the density of states (DOS). A high DOS at a specific energy level indicates many available states for occupation at that energy (Asefa & Gerbaba, 2022). The band arrangement and density of states for the Al_2O_3 sample are presented in Figure 2(a & b). A detailed analysis of Figure 3(b & c) shows a significant contribution from the anion 2s-orbital hybrid to the lower valence band, while the anion 2p-orbital affects the upper valence band. Moreover, the cation 3p-orbital mainly contributes to the conduction band, as illustrated in Figure 3(c). The estimated bandgap value for corundum from Arusha mining indicates the insulating nature of the sample.

The estimated static dielectric constant ε_1 (0) for the corundum sample is 3.05 (Figure 4 a), whereby the value of the ordinary refractive index of 1.746 is obtained. This estimated value of the ordinary refractive index obtained using Figure 4(a) coincides with one that is indicated in Figure 4 (c). The refractive index obtained in this study is comparable to that of α-Al_2O_3 (Zouboulis & Grimsditch, 1991) of 1.774 value. The imaginary portion of dielectric function and extinction coefficient are also displayed in Figure 4(b & d). These results are in good agreement with the theoretical study (Feneberg et al., 2018). Therefore, it can be considered as the results that form the basis for further studies.

This suggests that the reflectivity is isotropic (uniform in all directions). The energy loss spectrum illustrates the amount of energy lost when a fast-moving electron traverses the material (Bouhemadou & Khenata, 2007). The bulk plasma frequency ω_p is the main peak on the loss function spectrum, this happens as $\varepsilon_2 < 1$ and ε_1 approach zero (Li et al., 2008). When comparing Figure 5(a), which shows a rapid decline in reflectance, to Figure 5(c), which features a sharp peak indicating a sudden drop in reflectance, the primary peak value in the loss function is approximately 25.10 eV (Figure 5c).

Elastic properties

The Arusha sample was observed to have smaller values of C_{11}, C_{12}, C_{13}, C_{33}, and C_{44} than the values from the literature. It appears that the Young's (G) modulus of elasticity for the Arusha sample is less than the value from the literature which indicates that the investigated corundum samples have low stiffness compared to values from the literature. In addition, at equilibrium pressure, the obtained elastic constants satisfy the criteria of stability for the rhombohedral phase:

$$C_{11} > |C_{12}|; \quad C_{13}^2 < \frac{1}{2}C_{33}(C_{11} + C_{12}); \quad C_{14}^2 + C_{15}^2 < C_{44}C_{66};$$

$$\text{where } C_{66} = \frac{C_{11} - C_{12}}{2}$$

From the calculated values in Table 2, Y is greater than B and G for the selected Arusha sample. Considering Pugh's ratio, the G/B ratio suggests that the Arusha sample is deemed brittle with a ratio of 0.65 with G/B > 0.5; and this sample has low Young's moduli in comparison to the theoretical values, which indicates that the material has low stiffness. The calculated Poison's ratio value from Table 2 is approximated to 0.23 indicating the dominant covalent bond in the Arusha sample.

Conclusion

The first principles studies technique was used to report the findings of electronic, optical, and elastic characteristics of α–Al_2O_3 in the corundum gemstones from the Arusha mining region. The findings correspond well with the known theoretical and experimental values. According to the findings, the reflectivity spectra showed isotropic behavior in the UV region. Furthermore, the results indicated that the selected corundum sample is a suitable insulator with a band gap of 6.13 eV. The selected sample

is deemed brittle with a ratio of 0.65 as G/B > 0.5; and it has low Young's moduli in comparison to the theoretical values, which indicates that the material has low stiffness. The calculated Poison's ratio value from the investigation is approximated to 0.23 indicating the dominant covalent bond in the Arusha sample.

Recommendations

There are still minor variations between the estimated optical spectra and the theoretical values, despite their good compatibility. Therefore, there is still much that can be learned about other features that will improve their applicability in several contemporary technologies by contrasting first-principles analyses of the electrical and optical properties of the corundum sample obtained from the Arusha mining zone with experimental findings. Studies on the temperature-dependent characteristic properties of the samples need to be undertaken. However, different techniques are required to study different properties of the corundum and compare the results with corundum from different parts of the world which can be found in literature. This can support much of its market and applications in different fields.

Acknowledgment

The authors gratefully acknowledge the Geological Survey of Tanzania (GST), Twiga Cement Industry, and the Department of Physics at the University of Dodoma for their contributions to this study.

References

Aggarwal, R. L., & Ramdas, A. K. (2019). *Physical properties of diamond and sapphire*. CRC Press.

Asefa Eressa, L., & Gerbaba Edossa, T. (2022). First-Principles Calculations to Investigate Structural, Electronic, Optical, and Elastic Properties of Ceria. *Advances in Condensed Matter Physics*, *2022, 1-11*.

Bouhemadou, A., & Khenata, R. (2007). Ab initio study of the structural, elastic, electronic and optical properties of the antiperovskite SbNMg3. *Computational Materials Science*, *39*(4), 803-807.

Clark, S. J., Segall, M. D., Pickard, C. J., Hasnip, P. J., Probert, M. I., Refson, K., & Payne, M. C. (2005). First principles methods using CASTEP. *Zeitschrift für kristallographie-crystalline materials*, *220*(5-6), 567-570.

Feneberg, M., Nixdorf, J., Neumann, M. D., Esser, N., Artús, L., Cuscó, R., Yamaguchi, T., & Goldhahn, R. (2018). Ordinary dielectric function of corundumlike α− Ga 2 O 3 from 40 meV to 20 eV. *Physical Review Materials*, *2*(4), 044601-044608.

Fischer, T. H., & Almlof, J. (1992). General methods for geometry and wave function optimization. *The Journal of Physical Chemistry*, *96*(24), 9768-9774.

Godin, T., & LaFemina, J. P. (1994). Atomic and electronic structure of the corundum (α-alumina)(0001) surface. *Physical Review B*, *49*(11), 7691-7696.

Heiba, Z., Mohamed, M. B., & Wahba, A. M. (2020). Structural, optical, mechanical, and electronic properties of Cr-doped alumina. *Journal of Materials Science: Materials in Electronics*, *31*, 14645-14657.

Karazhanov, S. Z., Ravindran, P., Kjekshus, A., Fjellvåg, H., & Svensson, B. (2007). Electronic structure and optical properties of Zn X (X= O, S, Se, Te): A density functional study. *Physical Review B*, *75*(15), 155104-155118.

Keulen, N., Thomsen, T. B., Schumacher, J. C., Poulsen, M. D., Kalvig, P., Vennemann, T., & Salimi, R. (2020). Formation, origin and geographic typing of corundum (ruby and pink sapphire) from the Fiskenæsset complex, Greenland. *Lithos*, *366*, 105536-105562.

Khireddine, A., Bouhemadou, A., Alnujaim, S., Guechi, N., Bin-Omran, S., Al-Douri, Y., Khenata, R., Maabed, S., & Kushwaha, A. (2021). First-principles predictions of the structural, electronic, optical and elastic properties of the zintl-phases AE3GaAs3 (AE= Sr, Ba). *Solid State Sciences*, *114*, 106563-106575.

Kovilpalayam Palaniswamy, D., Arumugan, P., Munusami, R., Chinnasamy, A., Madhu, S., Paulraj, P., & Palani, K. (2022). First Principles Study on Electronic Structure and Optical Properties of PMMA Doped

InSb–Mn Alloy Polymer Matrix Composite. *Advances in Materials Science and Engineering*, 2022, 1-6.

Li, C., Wang, B., Wang, R., Wang, H., & Lu, X. (2008). First-principles study of structural, elastic, electronic, and optical properties of orthorhombic BiGaO3. *Computational Materials Science*, *42*(4), 614-618.

Mansoor, M., Mansoor, M., Mansoor, M., Themelis, T., & Şahin, F. Ç. (2021). Sintered transparent polycrystalline ceramics: the next generation of fillers for clarity enhancement in corundum. *Synthesis and Sintering*, *1*(3), 183-188.

Ozaki, Y., Beć, K. B., Morisawa, Y., Yamamoto, S., Tanabe, I., Huck, C. W., & Hofer, T. S. (2021). Advances, challenges and perspectives of quantum chemical approaches in molecular spectroscopy of the condensed phase. *Chemical Society Reviews*, *50*(19), 10917-10954.

Park, H. (2004). *The gemological study of ruby and sapphire from Tanzania* MSc Thesis, Pukyong National University.

Perdew, J. P., Burke, K., & Ernzerhof, M. (1996). Generalized gradient approximation made simple. *Physical review letters*, *77*(18), 3865-3868.

Raisin, S. N., Jamaludin, J., Ismail, I., Wahab, Y. A., Rahim, R. A., Balakrishnan, S. R., Ismail, W. Z. W., Rahalim, F. M., Jamal, F. A. M., & Zaini, N. A. H. S. (2021). Simulation Study on CCD Tomography System for Ruby Stone Optical Properties. *Journal of Tomography System & Sensors Application, 4(1), 34-40*.

Vanderbilt, D. (1990). Soft self-consistent pseudopotentials in a generalized eigenvalue formalism. *Physical Review B*, *41*(11), 7892-7895.

Zainullina, V. M., & Korotin, M. A. (2020). Regulation of corundum band gap width by p elements and vacancy co-doping. *Journal of Physics and Chemistry of Solids*, *140*, 109357-109361.

Zouboulis, E., & Grimsditch, M. (1991). Refractive index and elastic properties of single-crystal corundum (α-Al2O3) up to 2100 K. *Journal of applied physics*, *70*(2), 772-776.